INDIAN JOURNAL OF SCIENCE AND TECHNOLOGY

RESEARCH ARTICLE

Check for updates

OPEN ACCESS

Received: 06-01-2022

Accepted: 19-05-2022

Published: 26-07-2022

Citation: Naduvinamani NB, Ganachari R (2022) Double-Layered Porous Rayleigh Step Slider Bearings Lubricated with Couplestress Fluids. Indian Journal of Science and Technology 15(28): 1389-1398. https://doi.org/10.17485/IJST/v15i28.33

* **Corresponding author**.

naduvinamaninb@yahoo.co.in

Funding: None

Competing Interests: None

Published By Indian Society for Education and Environment (iSee)

ISSN
Print: 0974-6846
Electronic: 0974-5645

Double-Layered Porous Rayleigh Step Slider Bearings Lubricated with Couplestress Fluids

N B Naduvinamani[1]*, Rakesh Ganachari[1]

1 Department of Mathematics, Gulbarga University, 585 106, Kalaburagi, INDIA

Abstract

Objective: To examine the performance of double-layered porous Rayleigh step slider bearings lubricated with couple stress fluid and to compare it with the performance of single layered porous Rayleigh step bearing. **Methods**: Based on the Stokes micro continuum theory of couple stress fluids, the modified Reynolds equation governing fluid film pressure is derived. Its analytical solution is and the closed form expressions for the fluid film pressure, frictional force and load carrying capacity are obtained. **Findings**: The numerical results for bearing characteristics such as pressure, load carrying capacity, frictional force are plotted graphically to study the effect of double-layered porous facing. The effect of permeability of the porous layer is to decrease the load carrying capacity as it gives an easy path for the lubricant to pass through. This adverse effect can be compensated by introducing double layered porous facing with different permeabilities and the results presented here in this paper clearly shows the increase in load carrying capacity and decrease in co-efficient of friction for the double layered porous bearings as compared to that of single layered porous bearings. **Novelty**: Original research was conducted on double-layered porous Rayleigh step slider bearings with couple stress fluid by considering the effects of lubricant additives in the porous region and the results are compared with that of single layered porous bearings.

Keywords: Doublelayered porous; Rayleigh-step slider bearing; Couple stress fluid; Microcontinuum; Permeability

1 Introduction

Rayleigh step bearings are capable of carrying the highest load carrying capacity as compared to many other slider bearings. Due to this, the step bearings found extensive applications in industry to improve the performance of automotive machines. The first study on step bearing was conceived in 1918 by Lord Rayleigh [(1)] with an objective of identifying the optimal shape with highest load capacity per unit width for a given film thickness and bearings length and now this configuration is named as Rayleigh step bearing. Since then several researchers analyzed this bearing configuration under various lubrication situations.

To mention a few, the thermo-elasto-hydrodynamics lubrication simulation of Rayleigh step bearing using the progressive mesh densification method was analyzed by Kumar et.al [2]. The effects of longitudinal surface Roughness on the performance of Rayleigh step bearing was studied by Andharia and Pandya [3]. Distribution of recirculation and pressure in a Rayleigh step bearing was studied by Feng et. al. [4]. Naduvinamani and Patil [5] analyzed the problem of Magnetohydrodynamics effect on the static and dynamic characteristics of couple stress fluid lubricated Rayleigh step bearings. Rahul Kumar et.al. [6] made an attempt to analyze the effects of surface roughness on the performance of Rayleigh step bearing operating under thermo-elasto-hydrodynamic lubrication by considering the shear flow factor.

The use of different fluids with additives of high molecular weight polymers to improve the viscosity index of lubricants is considered. Mouda et.al [7] studied the effects of non-Newtonian magneto-elasto-hydrodynamics on the performance of slider-bearings. Viorel Badescu [8] analyzed the problem of two classes of sub-optimal shapes for one dimensional slider bearings with couple stress lubricants. Mouda et.al. [9] studied the effects of surface roughness on the non-Newtonian squeeze film characteristics between parallel plates.

Bujurke et.al. [10] analyzed the problem of porous Rayleigh step bearing lubricated with non-Newtonian second–order fluid by considering the Darcy's equations for the flow of fluid in the porous region. Naduvinamani and Siddangouda [11] studied the problem of porous Rayleigh step bearing with couple stress fluids by modeling the flow of couple stress fluid in the porous region by modified Darcy's law which takes in to account of microstructure additives in the lubricant. Bhattacharjee et.al [12] conducted the theoretical study on the single-layered porous short journal bearing with micropolar fluid. In all these studies it is observed that, the effect of single layer porous facing on the bearing surface is to reduce the load carrying capacity. Naduvinamani and Shridevi [13] studied the static and dynamic characteristics of porous plane inclined slider bearings lubricated with magneto-hydrodynamic couple stress fluid. Hanumagowda et.al. [14] Studied the effect of magneto-hydrodynamics and couple stresses on the steady and dynamic characteristics of porous exponential slider bearings. Rao and Agarwal [15] studied the problem of the effects of couple stresses on the performance of rough step slider bearings with assorted porous structure. The design of porous step bearing studied by Patel et.al [16] by considering different Ferro-fluid lubrication models. An excellent review of the design and optimization of large-scale hydrostatic bearing systems was given by Michal Michalec et.al [17]. A bearing load carrying capacity can be increased by reducing the seepage in to the wall of the bearing. This can be accomplished by reducing the permeability of the porous wall.However, this is impractical because a reduction in the permeability is accompanied by a reduction in the porosity and thus by a reduction in the oil content within the bearing material.

Uma Srinivasan [18] analyzed the problem of double-layered porous slider bearings and found that the effects of the presence of double-layered porous facing on the bearing surface is to increase the load capacity and the frictional force but to reduce the coefficient of friction as compared the conventional porous bearings. Characteristics of double-layered porous micropolar fluid lubricated journal bearing is studied by Bhattacharjee *et. al,* [19]. The non-Newtonian effects of second– order fluids on double-layered porous Rayleigh-step bearings was studied by Naduvinamani [20] and found that the for the optimal load carrying capacity the step height ratio and the bearing lengths are smaller for the double layered porous bearing as compared to that of conventional porous Rayleigh step bearings. The analysis of journal bearing with double-layered porous lubricant film by considering the effects of surface porous layer configuration was studied by Rao et.al. [21]. In their study it is found that the load carrying capacity increases significantly for increasing values of non-dimensional porous layer thickness couple stress parameter. Singh and Sharma [22] studied the combined effects of wear and non-Newtonian behavior of lubricant in the double-layered porous journal bearings.

A double-layered porous facing would be useful as it would not only increase the load capacity of the bearing because of reduced oil seepage into its wall but would also help to bring oil between the surfaces, thereby improving the performance of the bearing when it is not completely saturated with oil. Hence in this paper an attempt has been made to analyze the double-layered porous step-slider bearing lubricated with couple stress fluid which has not been studied so far. Results are compared with that of single-layered porous step-slider bearing analyzed by Naduvinamani and Siddangouda [11]. The numerical results are presented in the graphical form. The presented results show that the introduction of the double-layer porous facing increases the load carrying capacity and frictional force however decreases the co-efficient of friction which are the desired attributes of efficient lubrication system. This investigation bridges the gap of study between the single layered porous Rayleigh step bearing and double layered bearings.

2 Nomenclature

$\bar{C}_f$ non-dimensional coefficient of friction.

$\overline{F}$ non-dimensional frictional force

h film thickness

h_1 thickness of inlet film
h_2 thickness of outlet film
k porous matrix permeability
L bearing length (=L_1+L_2)
L_1, L_2 Bearing lengths in the entry and exit regions respectively
l couple stress parameter = $\left(\sqrt{\frac{\eta}{\mu}}\right)$
$\bar{l}$ non-dimensionalcouple-stress parameter
p pressure in film region
p_1^*, p_2^* fluid pressure in porous region-I and porous region-II
P Non-dimensional pressure = $\left(\frac{ph_2^2}{\mu U\ L}\right)$
P_1, P_2 Non-dimensional film pressure in the entry and exit region respectively.
u^* , v^* modified Darcy velocity in the x and y direction.
w load
$\overline{W}$ dimensionless load carrying capacity $= \left(\frac{wh_2^2}{\mu U\ L^2}\right)$
$\beta_{1.} = \left(\frac{\eta}{\mu}/k_1\right)$
$\beta_2 = \left(\frac{\eta}{\mu}/k_2\right)$
μ lubricant viscosity
η material constant for couple stresses
ψ permeability parameter = $\left(\frac{k_1\delta_1}{h_2^3}\right)$
δ_1, δ_2 thicknesses of porous layer-1 and porous layer-2 respectively
k_1, k_2 permeabilities in the layer-1 and porous layer-2 respectively

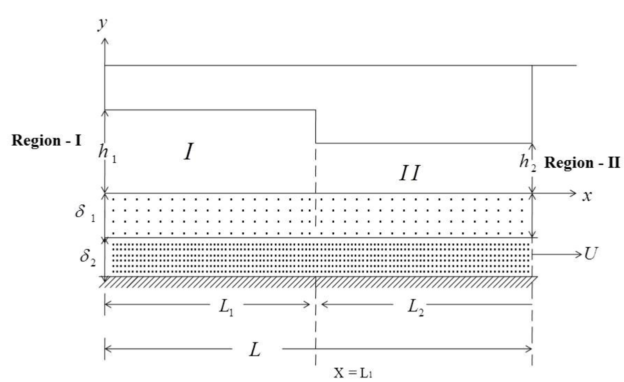

Fig 1. Double – layered porous Rayleigh step bearing

3 Mathematical formulation

The governing equations for the Stokes couple stress fluid are given by[11]

$$\frac{\partial u}{\partial x} + \frac{\partial v}{\partial y} = 0 \tag{1}$$

$$\mu \frac{\partial^2 u}{\partial y^2} - \eta \frac{\partial^4 u}{\partial y^4} = \frac{\partial p}{\partial x} \tag{2}$$

$$\frac{\partial p}{\partial y} = 0 \tag{3}$$

As shown in Figure 1 the surface profile for Rayleigh step bearing is determined by the mathematical function.

$$h(x) = \begin{cases} h_1 \text{ for } 0 < x < L_1, (\text{ Region } -I) \\ h_2 \text{ for } L_1 < x < L (\text{ Region } -II) \end{cases}$$

Bearing length (L) is equal to the sum of the lengths of entry and exit regions (=L_1 +L_2). The velocity boundary conditions are

1. at $y = h$

$$u = 0, \frac{\partial^2 u}{\partial y^2} = 0 \tag{4a}$$

$$v = 0 \tag{4b}$$

2. at $y = 0$ (on the porous surface)

$$u = U, \frac{\partial^2 u}{\partial y^2} = 0 \tag{5a}$$

$$v = -v^* \tag{5b}$$

Assuming that v^* is the Darcy's velocity component carried along y axis in the porous region. Couple stress fluid flows within the porous region according to Darcy's modified law

$$u^* = \frac{-k_1}{\mu(1-\beta_1)} \frac{\partial p^*}{\partial x} \tag{6}$$

$$v^* = \frac{-k_1}{\mu(1-\beta_1)} \frac{\partial p^*}{\partial x}, \tag{7}$$

where k_1, k_2 are the permeability parameters of porous layer-1 and layer-2 respectively $\beta_1 = \left(\frac{\eta}{\mu}/k_1\right)$ and $\beta_2 = \left(\frac{\eta}{\mu}/k_2\right)$ are the ratio of microstructure size to the pore size. If $\left(\frac{\eta}{\mu}\right)^{\frac{1}{2}} \approx \sqrt{k_1}$, i.e. $\beta_1 \approx 1$.

Due to continuity of fluid flow in the porous regions, the pressure p_1^* in the porous layer-1 and p_2^* in the porous layer-2 are governed by the following equations [18]

$$\frac{\partial^2 p_1^*}{\partial x^2} + \frac{\partial^2 p_1^*}{\partial y^2} = 0 \tag{8a}$$

$$\frac{\partial^2 p_2^*}{\partial x^2} + \frac{\partial^2 p_2^*}{\partial y^2} = 0 \tag{8b}$$

The related pressure boundary conditions are

$$p_1^* = 0 \text{ at } x = 0 \text{ and } x = L \tag{9}$$

$$p(x,0) = p_1^*(x,0), \tag{10}$$

$$p_1^*(x,-\delta_1) = p_2^*(x,-\delta_1), \tag{11}$$

$$\left(\frac{\partial p_2^*}{\partial y}\right)_{y=-(\delta_1+\delta_2)} = 0 \tag{12}$$

$$\frac{k_1}{\mu(1-\beta_1)}\left(\frac{\partial p_1^*}{\partial y}\right)_{y=-\delta_1} = \frac{k_2}{\mu(1-\beta_2)}\left(\frac{\partial p_2^*}{\partial y}\right)_{y=-\delta_1} \tag{13}$$

Integrating Eq. (8a) with respect to y over the wall thickness

$$\left(\frac{\partial p_1^*}{\partial x}\right)_{y=0} = -\int_{-\delta_1}^{0}\frac{\partial p_1^*}{\partial x^2}dy + \left(\frac{\partial p_1^*}{\partial y}\right)_{y=-\delta_1} \tag{14}$$

Integrating Eq. (8b) with respect to y over the wall thicknessuse of Eq. (13) gives

$$\left(\frac{\partial p_1^*}{\partial y}\right)_{y=0} = -\int_{-\delta_1}^{0}\frac{\partial p_1^*}{\partial x^2}dy - \frac{k_2(1-\beta_1)}{k_1(1-\beta_2)}\int_{-(\delta_1+\delta_2)}^{-\delta}\frac{\partial^2 p_2^*}{\partial x^2}dy \tag{15}$$

The wall thicknesses δ_1 *and* δ_2 to be small Eq.(15) reduces to

$$\left(\frac{\partial p_1^*}{\partial y}\right)_{y=0} = -\left(\delta_1 + \frac{k_2(1-\beta_1)}{k_1(1-\beta_2)}\delta_2\right)\frac{\partial^2 p^*}{\partial x^2}, \tag{16}$$

4 Solution of the problem

Equation (3) indicates that the pressure p in the film region is independent of y. Solving Eqn.(2) with relevant boundary conditions for u in equations (4a), (4b) and (5a), (5b), the fluid velocity in the film region is obtained in the form

$$u = U\left(1-\frac{y}{h}\right) + \frac{1}{2\mu}\frac{dp}{dx}\left[y^2 - yh + 2l^2\left\{1 - \frac{\cosh\left(\frac{2y-h}{2l}\right)}{\cosh\left(\frac{h}{2l}\right)}\right\}\right] \tag{17}$$

where $l = \sqrt{\frac{\eta}{\mu}}$ couplestress parameter

Using the expression for u given in Eq. (17) into the continuity equation (1) and integrating over the film thickness and using boundary conditions (4a), (4b) and (5a), (5b), we get the modified Reynolds equation

$$\frac{d}{dx}\left[\left[f_1(h,l)\frac{dp}{dx}\right] = 6\mu U\frac{dh}{dx} - \frac{12k_1}{(1-\beta_1)}\frac{\partial p_1{}^*}{\partial y}\right]_{y=0} \tag{18}$$

where

$f_1(h,l) = h^3 - 12l^2h + 24l^3\tanh(h/2l)$

Assuming that the double layered porous thickness to be very small, the Morgan-Cameron approximation gives

$$\left(\frac{\partial p_1^*}{\partial y}\right)_{y=0} = -\left(\delta_1 + \frac{k_2(1-\beta_1)}{k_1(1-\beta_2)}\delta_2\right)\frac{\partial^2 p}{\partial x^2} \tag{19}$$

Put Equation (19) in Eq.(18). Then the modified Reynolds –type equation is acquired in the form of

$$\frac{d}{dx}\left[\left\{f_1(h,l)-\frac{12k_1\delta_1}{(1-\beta_1)}\left(1+\frac{k_2(1-\beta_1)}{k_1(1-\beta_2)}\left(\frac{\delta_2}{\delta_1}\right)\right)\right\}\frac{dp}{dx}\right]=6\mu U\frac{dh}{dx} \tag{20}$$

Introducing the following non- dimensional quantities

$$\bar{x}=\frac{x}{L},\ p=\frac{ph_2^2}{\mu UL},\ \bar{l}=\frac{2l}{h_2^2},\ \psi=\frac{k_1\delta_1}{h_2^3},\ \bar{h}=\frac{h}{h_2},\ \overline{L_1}=\frac{L_1}{L},\ \overline{L_2}=\frac{L_2}{L} \tag{21}$$

Eq.(20) takes the form given below

$$\frac{d}{dx}\left[\left\{F(\bar{h},\bar{l})-\frac{12\psi}{1-\beta_1}(1+(KR)B_1)\right\}\frac{dP}{d\bar{x}}\right]=6\frac{d\bar{h}}{d\bar{x}}, \tag{22}$$

where

$$F(\bar{h},\bar{l})=\left[\bar{h}^3-3\bar{l}^2+3\bar{l}^3\tanh(\bar{h})\right] \tag{23}$$

$KR=\frac{k_2}{k_1}, B_1=\left(\frac{1-\beta_1}{1-\beta_2}\right)\left(\frac{\delta_2}{\delta_1}\right)$

The fluid film pressure boundary conditions are

$$p=0\ \text{ at }\ \bar{x}=0;\quad p=p_c\ \text{ at }\ \bar{x}=\overline{L_1} \tag{24}$$

Here $p_c$is the non–dimensional pressure at the step. Integrate Eq. (22) twice with respect $\bar{x}$ tousing boundary conditions (24) the fluid film pressure is obtained in the form

$$p_c=6\left\{\frac{\overline{h_1}-\bar{h}_m}{F(\bar{h},\bar{l})-\frac{12\psi}{1-\beta_1}(1+(KR)B_1)}\right\}\overline{L_1}\ \text{ for entry region} \tag{25}$$

$$p_c=6\left\{\frac{\overline{h_m}-1}{F(\bar{h},l)-\frac{12\psi}{1-\beta_1}(1+(KR)B_1)}\right\}\overline{L_2}\ \text{ for exit region} \tag{26}$$

From Equations (25) and (26), we get

$$\overline{h_m}=\frac{\bar{h}_1\bar{L}_1\left(F\left(\bar{h}_1,\bar{l}\right)\right)-\frac{12\psi}{1-\beta_1}(1+(KR)B_1)+\bar{L}_2\left(F\left(\bar{h}_1,\bar{l}\right)\right)-\frac{12\psi}{1-\beta_1}(1+(KR)B_1)}{\bar{L}_2\left(F\left(\bar{h}_1,\bar{l}\right)\right)-\frac{12\psi}{1-\beta_1}(1+(KR)B_1)+\bar{L}_1\left(F\left(\bar{h}_1,\bar{l}\right)\right)-\frac{12\psi}{1-\beta_1}(1+(KR)B_1)} \tag{27}$$

Now the pressure for the entry region (0≤ $\bar{x}\le\overline{L_1}$) is

$$P_1=6\left[\frac{\bar{L}_2\left(\bar{h}_1-1\right)}{\overline{L_2}\left(F\left(\overline{h_1},\bar{l}\right)\right)-\frac{12\psi}{1-\beta_1}(1+(KR)B_1)+\bar{L}_1\left(F\left(\overline{h_1},\bar{l}\right)\right)-\frac{12\psi}{1-\beta_1}(1+(KR)B_1)}\right]\bar{x} \tag{28}$$

$P_1=6\left[\frac{-L_2\left(\overline{h_1}-1\right)}{\overline{L_2}\left(F\left(\overline{h_1},\bar{l}\right)\right)-\frac{12\psi}{1-\beta_1}(1+(KR)B_1)+\overline{L_1}\left(F\left(\overline{h_1,l}\right)\right)-\frac{12\psi}{1-\beta_1}(1+(KR)B_1)\right]}\right]$

For the exit region ($\le\bar{x}\le 1$) is

$$P_2=6\left[\frac{\overline{L_1}\left(\overline{h_1-1}\right)}{\overline{L_2}\left(F\left(\overline{h_1,l}\right)\right)-\frac{12\psi}{1-\beta_1}(1+(KR)B_1)+\bar{L}_1\left(F\left(\overline{h_1,l}\right)\right)-\frac{12\psi}{1-\beta_1}(1+(KR)B_1)}\right]\bar{x} \tag{29}$$

Using Eqs.(28) and (29) we get the non-dimensional load carrying capacity.

$$\bar{W} = \frac{wh_2^2}{\mu U\, L^2} = 3\left[\frac{\bar{L}_1\left(\bar{L}_1\right)\left(\bar{L}_2-\bar{L}_1+1\right)+\left(\bar{h}_1-1\right)}{\bar{L}_2\left(F\left(\bar{h}_1,\bar{l}\right)\right)-\frac{12\psi}{1-\beta_1}\left(1+(KR)B_1\right)+\bar{L}_1\left(F\left(\bar{h}_1,\bar{l}\right)\right)-\frac{12\psi}{1-\beta_1}\left(1+(KR)B_1\right)}\right] \tag{30}$$

The frictional force f per unit width on the bearing surface y = 0 is defined by

$$\bar{F} = \int_0^L \left(\tau_{yx}\right)_{y=0} dx \tag{31}$$

$$\tau_{yx} = \mu\frac{\partial u}{\partial y} - \eta\frac{\partial^3 u}{\partial y^3} \tag{32}$$

Put Eq. (18) into Eq.(33) and substituting it in Eq.(32) gives dimensionless frictional force $\overline{F}$, in the form

$$\overline{F} = \frac{-Fh_2}{\mu UL} = \int_0^1\left[\frac{1}{\overline{\overline{h}}}+\frac{\overline{h}}{2}\frac{dp}{d\overline{x}}\right]d\overline{x} \tag{33}$$

$$= \frac{\bar{L}_2A+\bar{L}_2B+\left(-1+\frac{1}{\bar{h}_1}\right)\bar{L}_1\left(\bar{L}_2A+\bar{L}_2B\right)+3\bar{L}_1\left(\bar{h}_1-1\right)\left(\bar{L}_2\bar{h}_1-1+\bar{L}_1\right)}{\bar{L}_2A+\bar{L}_2B} \tag{33}$$

where,

$$A = F\left(\bar{h}_1,\bar{l}\right)-\frac{12\psi}{1-\beta_1}\left(1+(KR)B_1\right)$$

$$B = F\left(1,\bar{l}\right)-\frac{12\psi}{1-\beta_1}\left(1+(KR)B_1\right)$$

The Coefficient of friction is computed as follows

$$\overline{C}_f = \frac{\overline{F}}{\overline{\overline{W}}} \tag{35}$$

5 Figures

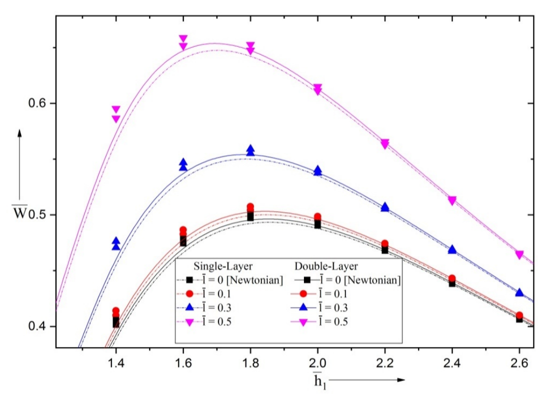

Fig 2. Variations of $\overline{W}$ with $\overline{h_1}$ for different values of $\bar{l}$ with fixed values of $\psi = 0.001,\ \overline{L}_1 = 0.7,\ \beta_1 = 0.3,\ \beta_2 = 0.6,$ KR $= 0.5,\ \delta_1 = 200,\ \delta_2 = 200$

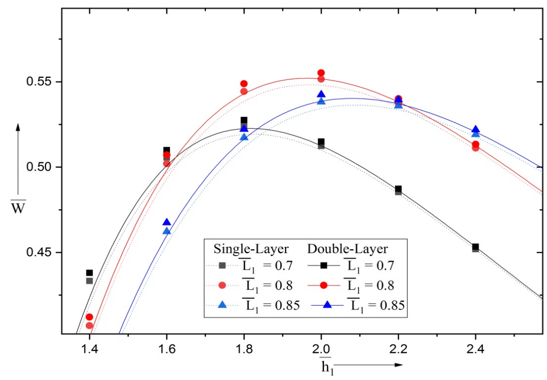

Fig 3. Variations of $\overline{W}$ with $\overline{h_1}$ for different values of $\overline{L}_1$ with fixed values of $\psi = 0.001,\ \bar{l} = 0.2,\ \beta_1 = 0.3,\ \beta_2 = 0.6,\ \mathrm{KR} = 0.5,\ \delta_1 = 200,\ \delta_2 = 200$

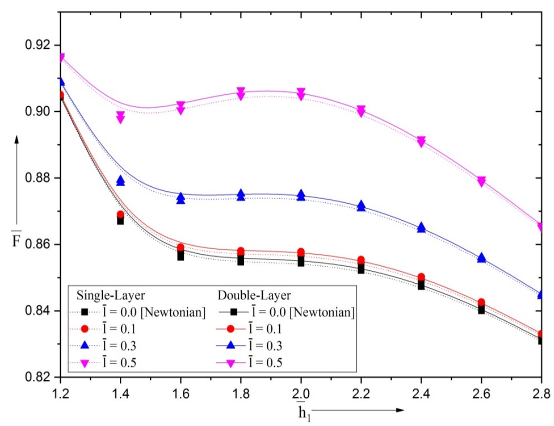

Fig 4. Variations of $\overline{F}$ with $\overline{h_1}$ for different values of $\bar{l}$ with fixed values of $\psi = 0.001,\ \overline{L}_1 = 0.7,\ \beta_1 = 0.3,\ \beta_2 = 0.6,\ \mathrm{KR} = 0.5,\ \delta_1 = 200,\ \delta_2 = 200$

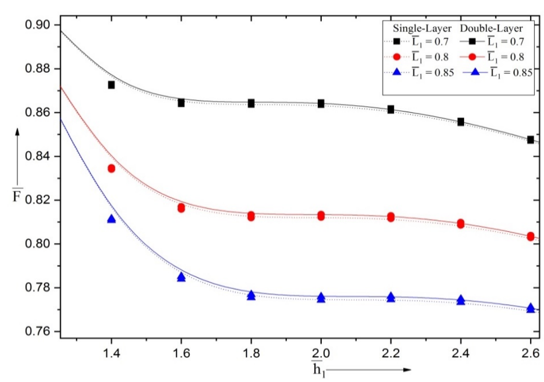

Fig 5. Variations of $\overline{F}$ with $\overline{h_1}$ for different values of $\overline{L}_1$ with fixed values of $\psi = 0.001,\ \bar{l} = 0.2,\ \beta_1 = 0.3,\ \beta_2 = 0.6,\ \mathrm{KR} = 0.5,\ \delta_1 = 200,\ \delta_2 = 200$

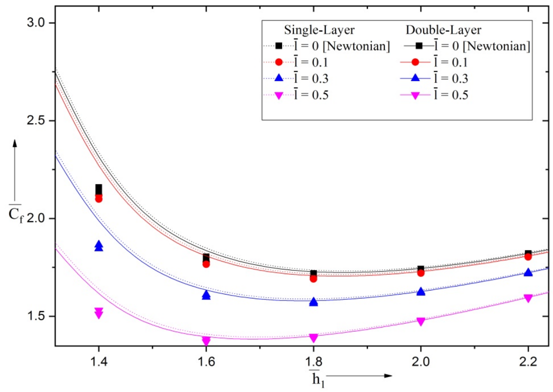

Fig 6. Variations of $\overline{C_f}$ with $\overline{h_1}$ for different values of $\bar{l}$ with fixed values of $\psi = 0.001, \bar{L}_1 = 0.7, \beta_1 = 0.3, \beta_2 = 0.6, \mathrm{KR} = 0.5, \quad \delta_1 = 200, \delta_2 = 200$

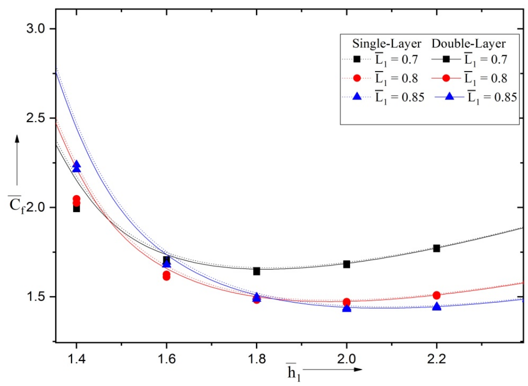

Fig 7. Variations of $\overline{C_f}$ with $\overline{h_1}$ for different values of $\bar{l}$ with fixed values of $\psi = 0.001,\ \bar{l} = 0.2,\ \beta_1 = 0.3,\ \beta_2 = 0.6,\ \mathrm{KR} = 0.5,\ \delta_1 = 200,\ \delta_2 = 200$

6 Results and Discussions

Load carrying capacity

Figure 2 shows the variance of non-dimensional load $\overline{W}$ different values of the couple stress parameter $\bar{l}$ for the constant values of ψ = 0.001, $\bar{L}$=0.7, β_1= 0.3, β_2= 0.6, KR=0.5, δ_1=200, δ_2=200. It is observed that, non-dimensional load carrying capacity increases for increasing the value of couple stress parameter $\bar{l}$. Further, it is evident that $\overline{W}$ increases for the double-layeredporous step-slider bearings as compared to that of single layered Rayleigh-step slider bearings. The most important aspect of the step bearing is to fix the step position for the optimum load carrying capacity. Hence in the Figure 3 variation of $\overline{W}$ with $\overline{h}_1$ for the different combinations of $\bar{L}_1$ and$\bar{L}_2$ it is observed that the maximum $\overline{W}$ with attained for $\bar{L}_1 = 0.8$ *and* $\bar{L}_2 = 0.2$ for both the cases.

The variation of non-dimensional frictional force $\bar{F}$ with $\bar{h}_1$ for different values of $\bar{l}$ and $\bar{L}_1$ is depicted in the Figures 4 and 5 respectively. It is observed the frictional force increases for the $\bar{l}$ and decreases for the increasing values of $\bar{L}_1$ Further, this increase in $\bar{F}$ is more accentuated for the double-layered porous bearings.

The key parameter to assess the performance of slider bearings is the coefficient of friction. The variation of the coefficient of friction $\bar{C}_f$ with $\bar{h}_1$ is plotted in the Figures 6 and 7 for various values of $\bar{l}$ and $\bar{L}_1$. It is observed that, the coefficient of friction decreases for the increasing values of $\bar{l}$. It is observed that the coefficient of friction decreases with increasing values of $\bar{L}_1$ up to certain values of $\bar{h}_1$ and after that it increases.

7 Conclusions

The double-layered porous Rayleigh step-slider bearings lubricated with couplestress fluid is analyzed on the basis of Stokes couplestress fluid theory. Following conclusions are drawn on the basis of the numerical results presented in the above section:

1. The enhanced load carrying capacity of the double-layered porous Rayleigh step –slider bearing is observed as compared to that of single-layered porous bearings.

2. Even though the non-dimensional frictional force increases for the double layered porous Rayleigh step slider bearings, the coefficient of friction decreases.

3. The adverse effect of reduced load carrying capacity of the single layered porous Rayleigh step-slider bearing can be well compensated by the presence of double-layered porous facing with appropriable permeabilities.

References

1) Rayleigh OML. Notes on the theory of lubrication. *The London, Edinburgh, and Dublin Philosophical Magazine and Journal of Science*. 1918;35:205–205. Available from: https://doi.org/10.1080/14786440108635730.
2) Kumar R, Azam MS, Ghosh SK, Khan H. Thermo-elastohydrodynamic lubrication simulation of the Rayleigh step bearing using the progressive mesh densification method. *SIMULATION*. 2019;95(5):395–410. Available from: https://doi.org/10.1177/0037549718788727.
3) Andharia PI, Pandya HM. Effect of Longitudinal Surface Roughness on the Performance of Rayleigh Step Bearing. *International Journal of Applied Engineering Research*. 2018;13(21):14935–14976.
4) Shen F, Yan CJ, Dai JF, Liu ZM. Recirculation Flow and Pressure Distributions in a Rayleigh Step Bearing. *Advances in Tribology*. 2018;2018:1–8. Available from: https://doi.org/10.1155/2018/9480636.
5) Naduvinamani NB, Siddharam P. MHD effect on static and Dynamic characterstics of Rayleigh step slider bearings lubricated with couple stress fluid. *Journal of Advances Computing*. 2017;6(1):1–16. Available from: http://hdl.handle.net/10603/187105.
6) Kumar R, Azam MS, Ghosh SK. Influence of stochastic roughness on performance of a Rayleigh step bearing operating under Thermo-elastohydrodynamic lubrication considering shear flow factor. *Tribology International*. 2019;134:264–280. Available from: https://doi.org/10.1016/j.triboint.2019.01.025.
7) Mouda M, Nabhani M, Khlifi ME. Effect of non-Newtonian magneto-elastohydrodynamic on performance characteristics of slider-bearings. *Industrial Lubrication and Tribology*. 2019;71(10):1158–1165. Available from: https://doi.org/10.1108/ILT-11-2018-0416.
8) Badescu V. Two classes of sub-optimal shapes for one dimensional slider bearings with couple stress lubricants. *Applied Mathematical Modelling*. 2020;81:887–909. Available from: https://doi.org/10.1016/j.apm.2020.01.044.
9) Mouda M, Nabhani M, Khlifi ME. Surface roughness effects on non-Newtonian MHD non-parallel squeeze film bearing. *Industrial Lubrication and Tribology*. 2021;73(1):45–51. Available from: https://doi.org/10.1108/ILT-02-2020-0071.
10) Bujurke NM, Naduvinamani NB, Jagadeeswar M. Porous Rayleigh Step Bearing with Second-Order Fluid. *Zeitschrift für Angewandte Mathematik und Mechanik Volume 70, Number 11*. 1990;70:517–526.
11) Naduvinamani NB, Siddangouda A. A note on porous Rayleigh step bearings lubricated with couple-stress fluids. *Proceedings of the Institution of Mechanical Engineers, Part J: Journal of Engineering Tribology*. 2007;221(5):615–621. Available from: https://doi.org/10.1243/13506501JET206.
12) Bhattacharjee B, Chakraborti P, Choudhuri K. Theoretical analysis of single-layered porous short journal bearing under the lubrication of micropolar fluid. *Journal of the Brazilian Society of Mechanical Sciences and Engineering*. 2019;41(9). Available from: https://doi.org/10.1007/s40430-019-1861-1.
13) Naduvinamani NB, Shridevi S, Patil S. Static and Dynamic Characteristics of Porous Plane Inclined Slider Bearings lubricated with MHD Couple stress fluid. *Special Topics & Reviews in Porous Media: An International Journal*. 2018;9(4):313–328. Available from: http://hdl.handle.net/10603/249797.
14) Hanumagowda BN, Gonchigara T, Kumar JS, Kumar HM. Study of effect of magnetohydrodynamics and couple stress on steady and dynamic characteristics of porous exponential slider bearings. *Journal of Physics: Conference Series*. 2018;1000(1):012091. Available from: https://doi.org/10.1088/1742-6596/1000/1/012091.
15) Rao PS, Agarwal S. Theoretical Study of Couple Stress Fluid Film in Rough Step Slider Bearing with Assorted Porous Structures. *Journal of Nanofluids*. 2018;7(1):92–99. Available from: https://doi.org/10.1166/jon.2018.1420.
16) Patel DA, Joshi M, Patel DB. Design of porous step bearing by considering different Ferro Fluid lubrication flow models. *Journal of Manufacturing Engineering*. 1931;16(4):108–114. Available from: http://smenec.org/index.php/1/article/view/350.
17) Michalec M, Svoboda P, Křupka I, Hartl M. A review of the design and optimization of large-scale hydrostatic bearing systems. *Engineering Science and Technology, an International Journal*. 2021;24(4):936–958. Available from: https://doi.org/10.1016/j.jestch.2021.01.010.
18) Srinivasan U. The analysis of a double-layered porous slider bearing. *Wear*. 1977;42(2):205–215. Available from: https://doi.org/10.1016/0043-1648(77)90052-7.
19) Bhattacharjee B, Chakraborti P, Choudhuri K. Evaluation of the performance characteristics of double-layered porous micropolar fluid lubricated journal bearing. *Tribology International*. 2019;138:415–423. Available from: https://doi.org/10.1016/j.triboint.2019.06.025.
20) Naduvinamani NB. Non-Newtonian effects of second-order fluids on double-layered porous Rayleigh-step bearings. *Fluid Dynamics Research*. 1997;495:19–20. Available from: https://doi.org/10.1016/S0169-5983(97)00019-1.
21) Rao TVVLN, Rani AMA, Nagarajan T, Hashim FM. Analysis of Journal Bearing with Double-Layer Porous Lubricant Film: Influence of Surface Porous Layer Configuration. *Tribology Transactions*. 2013;56(5):841–847. Available from: http://dx.doi.org/10.1080/10402004.2013.801100.
22) Singh A, Sharma SC. Analysis of a double layer porous hybrid journal bearing considering the combined influence of wear and non-Newtonian behaviour of lubricant. *Meccanica*. 2021;56(1):73–98. Available from: https://doi.org/10.1007/s11012-020-01259-2.